INSTITUTE OF PHYSICS PUBLISHING NANOTECHNOLOGY
Nanotechnology **15** (2004) S684–S690 PII: S0957-4484(04)78331-2

Interfacing biological macromolecules with carbon nanotubes and silicon surfaces: a computer modelling and dynamic simulation study

S S Tatke[1], V Renugopalakrishnan[1,2,3] and M Prabhakaran[1]

[1] Bionanotechnology Group, Department of Biomedical Engineering, College of Engineering, Florida International University, Miami, FL 33174, USA
[2] Children's Hospital, Harvard Medical School, Boston, MA 02115, USA

E-mail: renu@biofold.net

Received 16 March 2004
Published 7 September 2004
Online at stacks.iop.org/Nano/15/S684
doi:10.1088/0957-4484/15/10/030

Abstract
Proteins are naturally occurring nanosystems, optimized by the process of evolution. Biotechnology of protein based nanostructures offers vast opportunities to re-engineer and combine them with other nanomaterials for technological applications. Our primary interest is to interface proteins like bacteriorhodopsin (bR) with carbon nanotubes and silicon surfaces for application in storage devices and biosensors. We have carried out extensive computer simulations to study the dynamics of carbon nanotubes and their interaction with proteins. The immobilization of the protein on the carbon nanotubes is carried out by either covalent bonding or aromatic π stacking. Our simulation studies reveal the difference between the π stacking and covalent bonding.

1. Introduction

Bionanotechnology exploits the unique properties of proteins to design protein-based nanodevices. The first step in this process, protein immobilization on surfaces of silicon and carbon nanotubes (CNTs), is to provide an anchoring platform in designing protein based nanodevices [1–4]. Micrometre-sized patterns of proteins, protein-arrays, have revolutionized proteomics. Micropatterns of proteins have also been created by first making patterned surfaces as templates. More precise positioning of proteins require microfabrication technologies such as scanning probe microscopy, scanning tunnelling microscopy, photolithography and atomic force microscopy [5]. The phenomenon of the self-assembly of proteins in lipids, driven by hydrophobic forces, provides a spontaneous cost-effective self-ordering of proteins in a lipid bilayer [6] which can be exploited relatively easily.

Molecular modelling and dynamics simulation play a crucial role in bionanotechnology by an exploration of the feasibility of any given anchoring platform. In the present molecular modelling and dynamics simulation study, we are exploring the possibility of using carbon nanotubes as anchoring platforms while simultaneously embarking on experimental studies of immobilizing proteins in our laboratory. Single walled CNTs are molecular wires that exhibit interesting structural, mechanical and electrical properties. This material is being viewed as a promising immobilization substrate because of its various characteristics, like significant mechanical strength, high surface area, excellent electrical conductivity and good chemical stability [7]. Computer modelling and simulation dynamics is used to derive the feasibility and relative merits of various immobilization platforms. In the present study, we are focusing on the immobilization procedures of proteins like bR [8], cytochrome C and glucose oxidase on the CNT.

[3] Author to whom any correspondence should be addressed.

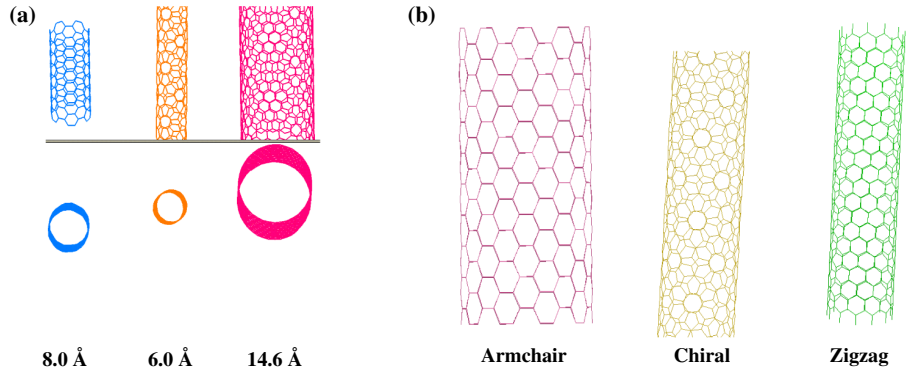

Figure 1. (a) Horizontal and vertical arrangements of CNT models. (b) Various types of CNT conformation.

2. Method

2.1. Single wall carbon nanotube (SWNT) simulations

CNTs of various sizes were generated using the program Tubegen [9]. Tubegen is a web based program, developed by Jeffrey T Frey at the University of Delaware. The user enters values for state variables such as the chirality of the nanotube, carbon–carbon bond length, export format and tube size. We have generated nanotubes of all three chiralities: armchair, zigzag and planar as well as tubes of various radii, as shown in figure 1. The program then generates the Cartesian coordinates of the nanotube structure. These coordinates are converted by into a PDB file using our in-house program MAK. This program, written in FORTRAN, takes the data generated by the algorithm as the input and generates an output file in the PDB format. RASMOL program [10] was used to view the generated nanotube structure.

The generated single wall nanotube structures were minimized using the Gromacs program [11], using our own potential function [12]. Most of the parameters were chosen from the Gromacs all atom potential. A special topology generating program was used to generate the topology of the molecule. The end effects were fixed by changing the atom type and changing them again after obtaining the final topology. After doing energy minimization a MD simulation was carried out for the CNT in solvent environment for 1 ns. The starting and final models of the simulation are shown in figure 2. These models show that the linearity of the CNT is more or less maintained, however the length of the tube was found to be less after the simulation was completed. The bonding distance of 1.423 Å was reduced to 1.23 Å due to the equilibration of the Gromacs potential values (figure 2). The primary parameter during the simulation is the bond length. Any change in the value of the bond length collapses the structure. A 1 ns trajectory analysis of the simulation was carried out. From the simulation we have calculated two parameters, the radius of gyration and the root mean fluctuation of the atoms. The former is a measure of the spread of the atoms from the centre and thereby a measure of atomic packing, whereas the later is a measure of atomic flexibility from the simulation. The radius of gyration plot, figure 3(a), shows the variation in the radius of gyration as a function of time. The plot shows that the nanotube has large fluctuations in the beginning and then shows a constant breathing motion after equilibration

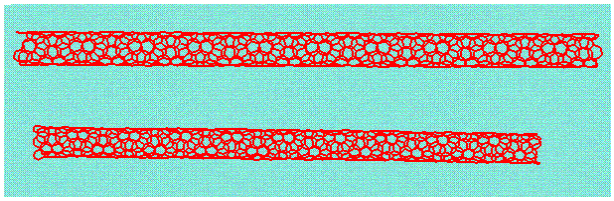

Figure 2. Change in length of the SWNT before and after MD simulation. Model parameters. Length before simulation = 110 Å. Length after simulation = 95 Å. Radius of tube before simulation = 6.26 Å. Radius of tube after simulation = 5.35 Å.

and shrinkage. The atomic RMS fluctuations (figure 3(b)) were also analysed as a function of the atom number. The calculated RMS fluctuations in figure 3(b) (fluctuations of the water not shown) show that the amplitude is largest at the ends and minimal at 1/4th the nanotube length. The increased flexibility in the middle is due to small bending motion. A similar observation has been reported by other workers [13, 14].

2.2. Multiwall carbon nanotube (MWNT) simulations

Similar simulations were also carried out for a multi wall carbon nanotube of outer radius 10 Å and inner radius 4 Å in solvent environment using the same parameters for 1 ns. Initially we noticed a large deformation in the outer tube due to the van der Waals' interactions between the two tubes. Then the bond length and the bond angle force constants were modified resulting in an increased rigidity of the tubes. However their attractive forces still dominate causing a deformation of the outer tube, though with a smaller magnitude. Next, we repeated the simulation in the absence of attractive van der Waals' force, similar to our tRNA simulation [15]. This resulted in the translational movement of the inner tube with respect to the outer tube. Using this knowledge we tuned the values for attractive and repulsive forces that would result in a stable MWNT structure after MD simulation. The starting model, the hydrated model during the simulation, and the final MWNT model are shown in figures 4(a)–(c), respectively. Two views of the models (figures 4(a) and (c)) show that there is a translational oscillation between the two tubes. The simulation shows some interesting features. The RMS fluctuations of the inner and outer tubes (figures 5(a), (b)) show similar behaviour. The amplitude of breathing motion is more evident in the

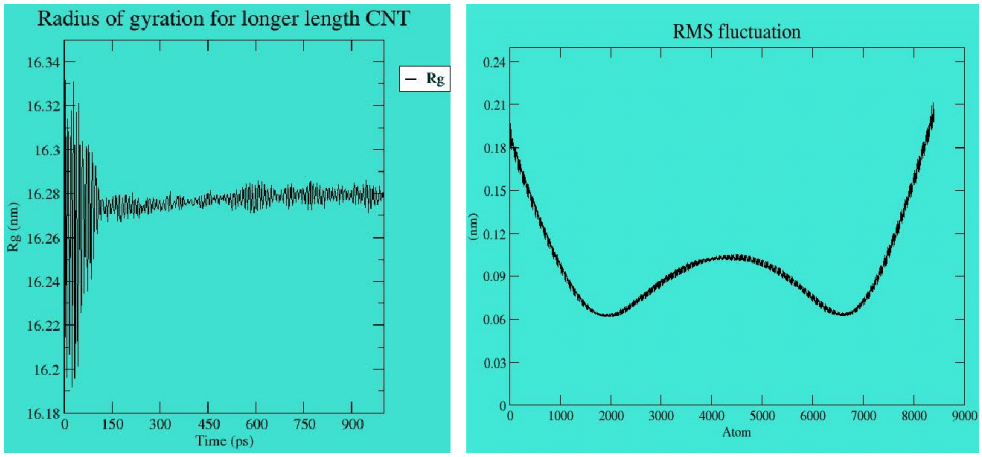

Figure 3. (a) Rg of the SWNT during MD simulation. (b) RMSF in the SWNT during MD simulation. Atom numbering is from one end of the CNT to another.

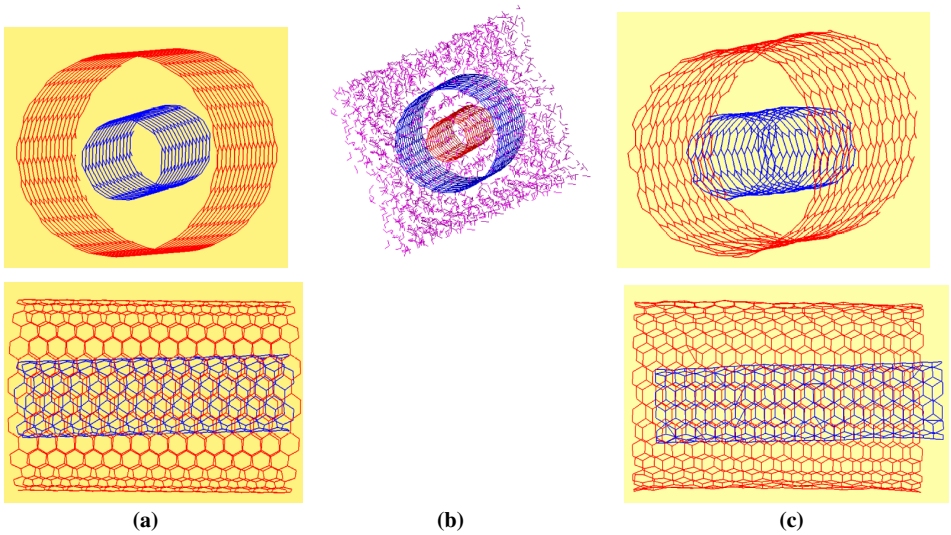

Figure 4. (a) Starting MWNT dimensions, outer radius: 10 Å, inner radius: 4 Å. (b) Hydration model box dimensions: $a = 35.36$ Å; $b = 35.36$ Å; $c = 50.70$ Å. (c) Final model.

outer tube as compared to the inner tube due to the restricted conformational space for the inner tube. We also analysed the packing pattern, in terms of radius of gyration, of both the inner (figure 5(c)) and outer tubes (figure 5(d)) separately and the complex (figure 5(e)). It was observed from the figures that the packing remains intact for individual tubes. They exhibit high frequency and low amplitude motions. The complex shows a large amplitude and low frequency motion due to relative collective movement between the two tubes, as shown in figure 5(e).

2.3. π stacking for interfacing biological macromolecules to the nanotube

Immobilization and visualization of DNA and proteins on CNT have been previously carried out [16–18]. π stacking and covalent bonds are two common types of bonds for interfacing biological macromolecules with the CNT. The π stacking approach is based on the presence of π bonds between the spacer (covalently bonded to protein) and the nanotube.

Figure 6(a) shows the CNT with a fused ring (spacer). The spacer contains four fused benzene rings to achieve sufficient π stacking with the CNT. Figure 6(b) show the spacer bonded to the cytochrome C system. The CNT, spacer and protein in a π stacking arrangement is shown in figure 6(c). Carbon rings are planar whereas the CNT rings are slightly curved due to their cylindrical nature. The difference in geometries presents a potential problem with regard to the interaction between the CNT and the carbon rings. However, because of the dynamic equilibrium, the planar ring has adequate interaction with CNT. In this method the spacer and the protein are physically bonded by a covalent bond, whereas the interaction between the spacer and the CNT is via the presence of π bonds between the spacer rings and the CNT rings. During our simulation only van der Waals' interaction and limited electrostatic forces are used to simulate the forces between the spacer ring and the CNT. The ring structure without covalent bonding to CNT remains stationary during its initial simulation. Next, a protein was added which was covalently linked to the spacer molecule. This π stacked system was subjected to a MD simulation for

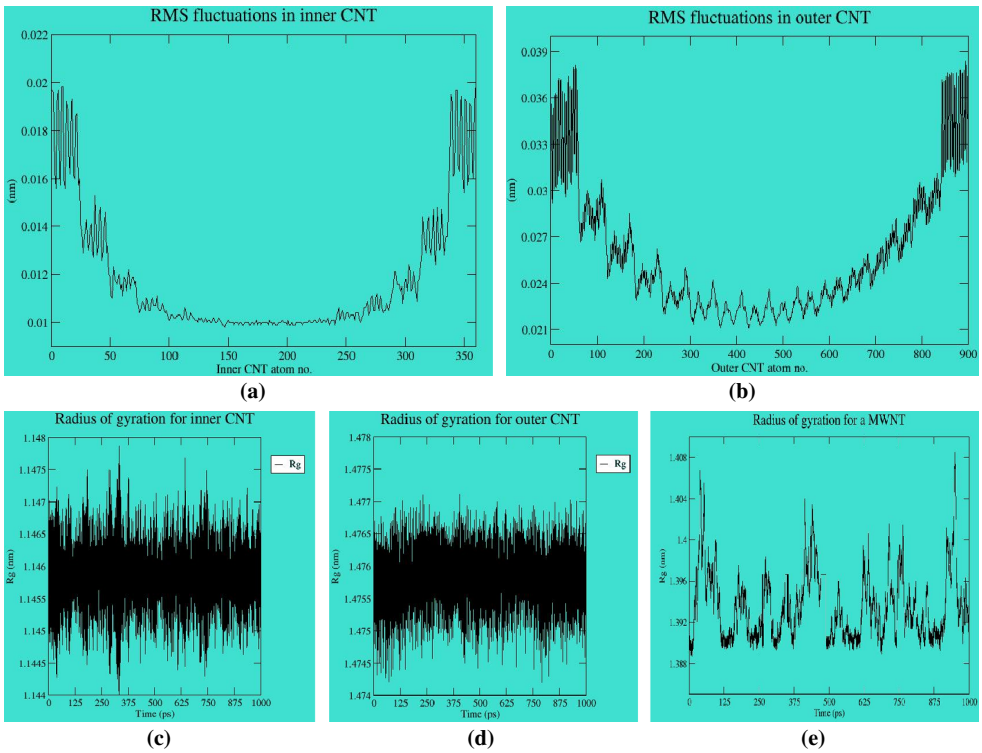

Figure 5. (a) RMSF in the inner nanotube of a MWNT during MD simulation. (b) RMSF in the outer nanotube of a MWNT during MD simulation. (c) Rg values for the inner nanotube of a MWNT during MD simulation. (d) Rg values for outer nanotube of a MWNT during MD simulation. (e) Rg values for a MWNT during MD simulation.

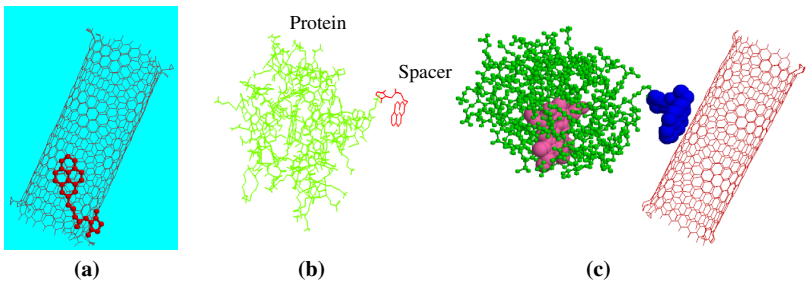

Figure 6. (a) CNT and four-ring spacer molecule. (b) Protein with spacer molecule bonded to it. (c) π Stacking arrangement with CNT, spacer and protein.

1 ns. The results are shown in figures 7 and 8. It was observed that, during the course of the simulation, the protein did not move the spacer away from the CNT. This establishes that π stacking is a feasible alternative to achieve interfacing between the macromolecule and the nanotube. The deformation of the CNT structure, mainly at the ends, occurs at 750 ps as shown in figure 7(b). The protein and the spacer remain intact during the entire simulation. The CNT shows normal breathing motion with the end effects clearly visible from figure 7(b). Another interesting feature noticed was the RMS fluctuation; figure 8(b) showing the amplitude of oscillation is not uniform with the cylinder, similar to the earlier results.

2.4. Covalent bonding for interfacing biological macromolecules to the nanotube

Covalent bonding [19] is an alternative approach to π stacking wherein the sensor protein is linked to the CNT through an intermediate linker molecule. Figure 9 shows the arrangement between CNT, linker and protein in a covalent bonding arrangement. The length of the linker molecule can be varied. The topology of the linker molecule was obtained using the PRODRG program [20]. This program accepts small molecules as input in the PDB format and generates molecular topologies using these coordinates. One side of the linker molecule was covalently connected to the CNT. The other side was connected to the surface positive residues (Lys and Arg) of the protein, also by a covalent bond. The protein was connected to the CNT by four sequential bonds. These new bonds are mostly single bonds which introduces some flexibility on the protein. Our MD simulations results are shown in figures 10 and 11. They show that both the CNT and the protein remain intact and the overall structure is preserved as revealed by calculations of radius of gyration (figure 10) and RMS fluctuations (figure 11). The end effect is clearly visible. We expected abnormal behaviour at the linking region (near

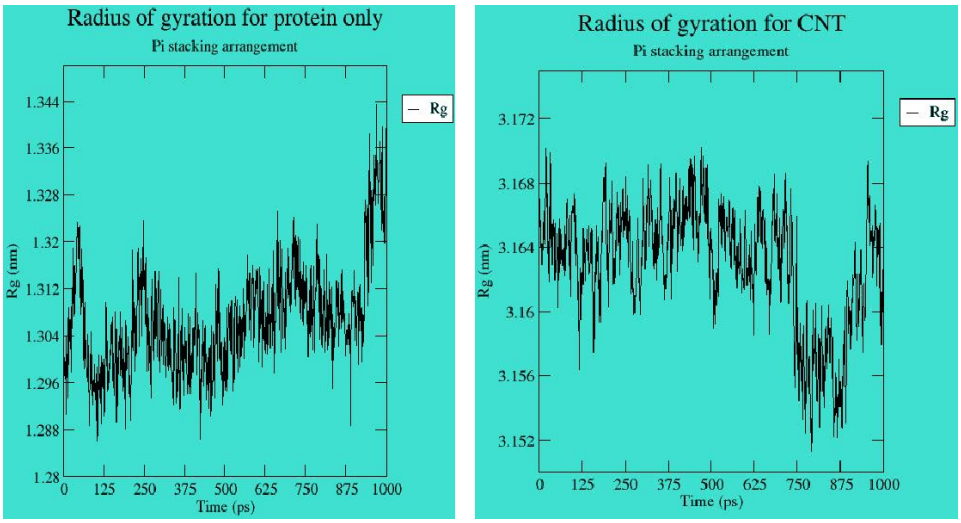

(a) **(b)**

Figure 7. (a) Rg values of protein alone in a π stacking arrangement during MD simulation. (b) Rg values for CNT alone in a π stacking arrangement during MD simulation.

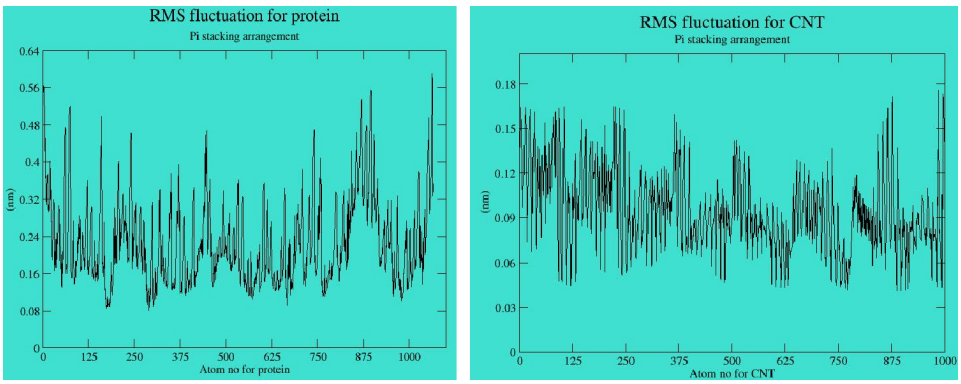

(a) **(b)**

Figure 8. (a) RMSF values for protein in a π stacking arrangement. (b) RMSF values for CNT in a π stacking arrangement.

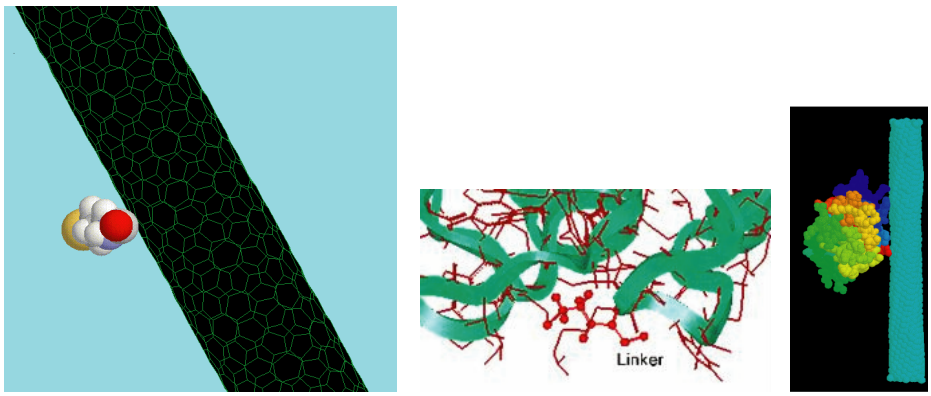

(a) **(b)** **(c)**

Figure 9. (a) CNT covalently linked to a spacer. (b) Linear linker bonded to a Cys residue molecule (only partial protein is shown). (c) Covalently bonded arrangement of CNT, spacer and protein.

atom 166), but it was found to remain normal. The entire CNT structure remains intact through the simulation as revealed from Rg studies. The parabolic shape is in contrast to figure 3, where a bending motion was observed. The Rg of the protein and CNT shows normal oscillations. The interesting feature is the general stabilizing effect of the attachment of high mass for both the systems. The RMSF plot values (figures 11(a), (b)) of both protein and CNT shows the restricted motion within the conformational space exhibiting low values in comparison with the π stacking simulation (figures 8(a) and (b)). When we

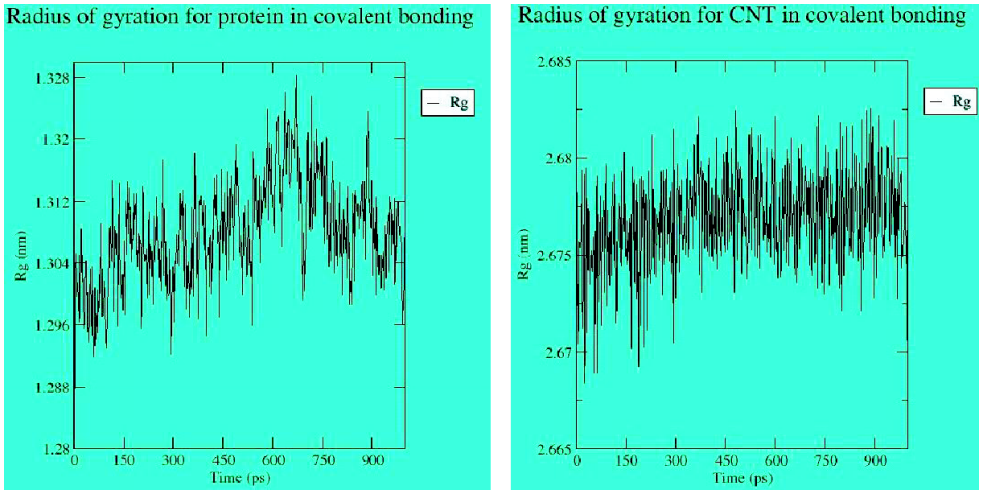

(a) **(b)**

Figure 10. (a) Rg values for protein alone in a covalent bonding arrangement during MD simulation. (b) Rg values for CNT alone in covalent bonding arrangement during MD simulation.

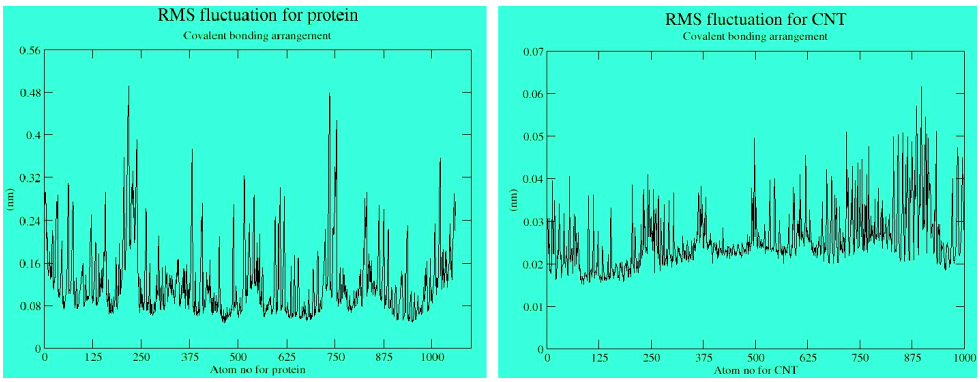

(a) **(b)**

Figure 11. (a) RMSF values for protein alone in a covalent bonding arrangement during MD simulation. (b) RMSF values for CNT alone in a covalent bonding arrangement during MD simulation.

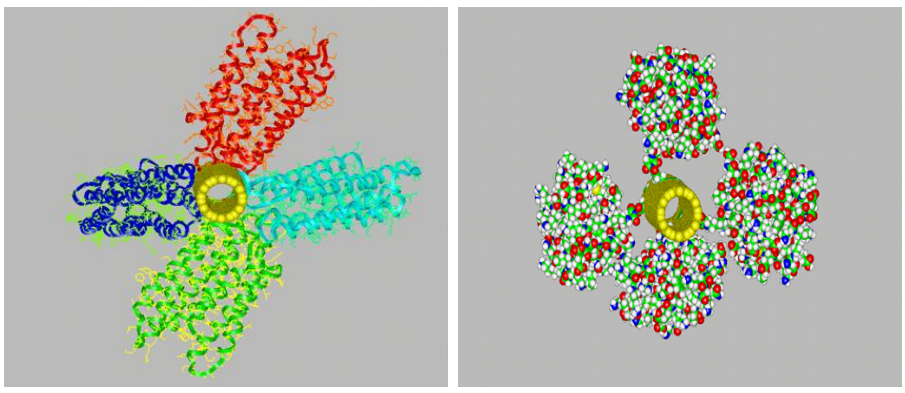

(a) **(b)**

Figure 12. (a) The vertical arrangement of bR over the CNT. The linker group's aromatic ring has π stacking with CNT and the Br was covalently linked to the thiolated group of the linker. (b) Glucose oxidase covalently attached to CNT.

have calculated the RMSF values for the whole system, they exhibit large values from the starting model due to oscillations in large Cartesian space.

We have also attempted to model the protein bR [21], used in storage devices, and glucose oxidase used in biosensors for monitoring blood glucose levels. The bR was linked by π stacking arrangement (figure 12(a)) and glucose oxide was covalently attached (figure 12(b)).

Both the simulation and modelling supplements the advantage of π stacking over covalent bonding. The π stacking

provides more freedom for the heme group to interact with the CNT for effective electron conductance in the design of bionanosensors. The breathing motion seems more suitable for π stacking interactions. Retaining the intactness of the protein is one of our main goals for designing a bionanosensor. The Rg values for π stacking (figure 7(a)) and covalent bonding (figure 10(a)) shows that this is easily achieved in both π stacking as well as covalent bonding. By using a vertical arrangement, more proteins can be accommodated with CNT surface as shown in figure 12, thereby increasing the signal to noise (S/N) ratio in the bionanosensor.

3. Conclusion

The dynamic nature of single walled and multi walled nanotubes in terms of Rg and RMSF values derived from 1 ns simulations were highlighted in this study. The interaction of CNT with proteins both by π stacking and covalent bonding was brought out. The computer models provide additional information on the accommodation of proteins with CNT.

Acknowledgments

We acknowledge a grant from Air Force (AFOSR grant no. FA9550-04-1-0098). Authors would like to express their thanks to Florida International University, Miami, FL, USA for financial support of the research described in this paper.

References

[1] Fields S 2001 *Science* **291** 1221
[2] Gilardi G 2001 *Trends Biotechnol.* **19** 468–76
[3] Zhu H and Snyder M 2001 *Curr. Opin. Chem. Biol.* **5** 40
[4] MacBeath G 2001 *Nat. Biotechnol.* **19** 828
[5] Hodneland C D, Lee Y-M, Min D-H and Mrksich M 2002 *Proc. Natl Acad. Sci. USA* **99** 5048
[6] Rytomaa M and Kinnunen P K 1994 *J. Biol. Chem.* **269** 1770–4
[7] Halwa N S (ed) *Handbook of Nanostructured Materials and Nanotechnology vol 5 Organics Polymers and Biological Materials* (CA: Academic Press)
[8] Pavlovic E, Quist A P, Gelius U, Nyholm L and Oscarsson S 2003 *Langmuir* **19** 4217–21
[9] Frey J T and Doren D J 2003 *TubeGen* (Newark, DE: University of Delaware) http://deaddog.duch.udel.edu/∼frey/research/tubegenonline.html
[10] Sayle R A and Milner-White E J 1995 RasMol: Biomolecular graphics for all *Trends Biochem. Sci. (TIBS)* **20** 374.7
[11] Lindahl E, Hess B and van der Spoel D 2001 GROMACS: a package for molecular simulation and trajectory analysis *J. Mol. Mod.* **7** 306–17
[12] Prabhakaran M, Gursahani S H, Verma C S, Garduno-Juarez R and Renugopalakrishnan V 2004 *J. Phys. Chem. Solids* **65** 1615–22
[13] Shrivastava D and Barnard S 1997 *Proc. IEEE Supercomputing '97* (Los Alamitos, CA: IEEE Computer Society Press)
[14] Yakobson B I, Brabec C J and Bernholc J 1999 *Phys. Rev. Lett.* **83** 273
[15] Prabhakaran M, Harvey S C, Mao B and MacCammon J A 1983 *J. Biomol. Struct. Dyn.* **1** 357–69
[16] Frankland S J V, Cagler A, Brenner D W and Griebel M 2002 *J. Phys. Chem.* B **106** 3046
[17] Guo Z *et al* 1998 Immobilization and visualization of DNA and proteins on carbon nanotubes *Adv. Mater.* **10** 701–3
[18] Sotiropoulou S and Chaniotakis N A 2003 *Anal. Bioanal. Chem.* **375** 103–5
[19] Besteman K, Lee J-O, Wiertz F G M, Heering H A and Dekker C 2003 *Nano Lett.* **3** 727–30
[20] van Aalten D M F, Bywater R, Findlay J B C, Hendlich M, Hooft R W W and Vriend G 1996 PRODRG, a program for generating molecular topologies and unique molecular descriptors from coordinates of small molecules *J. Comput. Aided Mol. Des.* **10** 255–62
[21] Renugopalakrishnan V, Strzelczyk A, Li P, Mokhnatyuk A A, Gursahani S H, Nagaraju M, Prabhakaran M, Arjomandi H and Lakka S L 2003 *Int. J. Quantum Chem.* **95** 627–31